MitoFit Preprints 2022.17
doi:10.26124/mitofit:2022-0017
Open Access

Experimental Communication

Cite
Chicco AJ, Zilhaver PT, Whitcomb LA, Fresa KJ, Izon CS, Gonzalez-Franquesa A, Dometita C, Irving BA, Garcia-Roves PM (2022) Resolving the Rotenone Paradox: elucidating the complexity of multi-substrate respirometry protocols. MitoFit Preprints 2022.17. https://doi.org/10.26124/mitofit:2022-0017

Author contributions
AJC: designed and performed experiments, analyzed data, and wrote the manuscript
PTZ, LAW, KJF, CSI, AGF, CD: performed experiments and analyzed data
BAI, PMGR: designed and performed experiments, analyzed data, and edited the manuscript

Conflicts of interest
The authors declare they have no conflict of interest.

Received 2022-04-26
Accepted 2022-04-27
Online 2022-05-02

Data availability
Data available upon request

Keywords
Mitochondrial respiration, electron transport chain, succinate, glutamate, oxidative phosphorylation, high-resolution respirometry

Resolving the Rotenone Paradox: elucidating the complexity of multi-substrate respirometry protocols

Adam J Chicco[1], Philip T Zilhaver[1], Luke A Whitcomb[1], Kyle J Fresa[1], Cheyanne S Izon[1], Alba Gonzalez-Franquesa[2], Crystal Dometita[3], Brian A Irving[3,4], Pablo M Garcia-Roves[5]

1 Department of Biomedical Sciences, Colorado State University, Fort Collins, Colorado, USA;
2 NovoNordisk, Copenhagen, Denmark;
3 Geisinger Obesity Institute, Danville, Pennsylvania, USA;
4 Department of Kinesiology, Louisiana State University, Baton Rouge, Louisiana, USA;
5 Department of Physiological Sciences, University of Barcelona, Barcelona, Spain

* Corresponding authors: adam.chicco@colostate.edu

Abstract

Multi-substrate respirometry protocols are frequently used to resolve the relative contributions of NADH-producing (N-pathway or CI-linked) substrates and succinate (S-pathway or CII-linked substrate) to mitochondrial oxygen consumption rate (J_{O_2}). Similarly, rotenone (a selective CI inhibitor) is utilized in the presence of N+S substrates to deduce the contribution of N-pathway flux to the total (N+S-pathway) J_{O_2}. However, under S- and some N+S pathway states, rotenone elicits a paradoxical increase in J_{O_2}, revealing a complex interaction of N- and S-pathway substrate oxidation on J_{O_2} *in vitro*. Herein, we demonstrate inhibitory effects of >1 mM malate or malonate (a CII inhibitor) on J_{O_2} supported by pyruvate and/or glutamate, suggesting that endogenous succinate oxidation interacts with malate concentration to potently regulate J_{O_2} supported by N-pathway substrates in a tissue-specific manner. Potential mechanisms are discussed to stimulate further experimentation aimed at elucidating the biological bases for variations in NS-pathway flux in multi-substrate respirometry protocols.

1. Introduction

The mitochondrial electron transfer system (ETS) plays a central role in cellular metabolism and redox biochemistry by facilitating the oxidation of reducing equivalents utilized in oxidative phosphorylation (OXPHOS) and a diverse array of catabolic and anabolic pathways. Complex I (NADH Dehydrogenase; CI) is the primary site of electron entry to the ETS, ultimately facilitating the oxidation of carbohydrate, fatty acid, and amino acid fuels. As electrons are transferred from NADH to ubiquinone, CI transfers some of their potential energy to pump protons (H^+) from the mitochondrial matrix into the intermembrane space, contributing to the development of the proton motive force (*pmF*) that powers ATP synthesis. As the primary site of mitochondrial NADH oxidation, CI also regulates levels of NAD^+ utilized for the oxidation of most carbon energy sources and anaplerotic substrates in the tricarboxylic acid cycle (TCA; Figure 1A). Complex II (Succinate Dehydrogenase; CII) transfers electrons from succinate to ubiquinone without pumping protons into the intermembrane space but participates directly in the TCA cycle by generating fumarate. Therefore, complete oxidation of substrates by the conventional TCA cycle requires both CI and CII activities, but the relative contributions of each complex depend on the stoichiometries of enzyme expression, the entry points, and concentrations of anaplerotic substrates being oxidized, and the allosteric regulation of enzymes involved.

Determining the discrete contributions of Complexes I and II to metabolic flux can provide insight into how mitochondria regulate cellular responses to physiological and pathological stress. This is commonly achieved by monitoring the effect of selective CI or CII substrates and inhibitors on mitochondrial respiration in vitro. High-resolution respirometry (HRR) enables stepwise evaluation of oxygen consumption rates (J_{O_2}) in mitochondrial preparations to titrations of anaplerotic substrates that feed the TCA cycle at different sites (Gnaiger 2020). Substrates that are directly oxidized by NAD-dependent enzymes, including pyruvate, glutamate, and malate, are conventionally considered to be "CI-linked", supplying electrons to the ETS through oxidation of NADH (the "N-pathway"). Succinate supports J_{O_2} through the supply of electrons through the succinate dehydrogenase complex (CII-linked or "S-pathway"). Electrons from CI and CII both reduce ubiquinone (Q) in the inner mitochondrial membrane, leading to a convergence of electron flow at the "Q-junction" that determines the net flow of electrons to Complex III and ultimately O_2 at Complex IV.

A simplistic view of this convergence predicts that electron flow from N-pathway substrates sum with succinate (S-pathway) electrons to account for 100% of the integrated J_{O_2} resulting from TCA cycle flux and related oxidation reactions upstream (Figure 1B). The contributions of each pathway can thus be revealed by monitoring J_{O_2} following sequential titration of N- and S-linked substrates or by the selective inhibition of CI or CII following stabilization of combined N+S pathway flux (Figure 1C). Indeed, this is the conventional interpretation of data from HRR protocols, leading to the use of substrate-control factors to describe the relative contributions of N and S pathway across a range of tissue and conditions (Gnaiger 2020). However, titrating millimolar concentrations of N- and S-pathway substrates can also lead to allosteric or feedback inhibition of TCA cycle enzyme activities and cataplerosis of TCA cycle intermediates, which can impact substrate oxidation rates and complicate interpretation of HRR protocols (Chance, Hagihara 1962; Harris, Manger 1968; Gnaiger 2020). While such interactions are difficult to predict and explain, careful systemic experimentation across

sample types, species, and conditions has the potential to reveal novel control points of TCA cycle flux and cellular bioenergetics with broad relevance to basic biology and disease processes. Accordingly, the primary aim of this study and "living publication" is to elucidate the basis for these interactions by providing a platform for the presentation and discussion of such experiments, beginning with an early observation that highlights the complexity and tissue-specificity of N and S pathway interactions on integrated J_{O_2} in multi-substrate respirometry protocols.

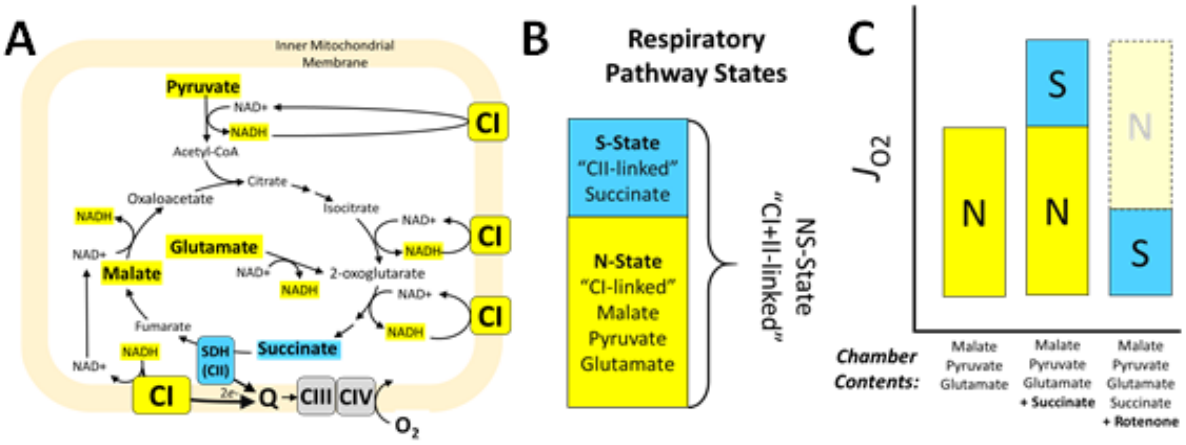

Figure 1. Simplistic view of mitochondrial substrate-linked respiratory states. A) Canonical illustration of citric acid cycle (CAC) flux and with sites of NADH production and succinate oxidation that support electron entry to the electron transfer system at Complexes I and II. B) Conventional classification of NADH-linked (N-state; yellow) and succinate-linked (S-state; blue) respiration states, and C) how multi-substrate titration protocols are frequently used to deduce their respective contributions to mitochondrial oxygen consumption rate (J_{O_2}).

2. Methods

2.1. Sample preparation and High Resolution Respirometry

Samples were obtained from male mice obtained from FVB, and C57Bl/6 mouse colonies maintained at Colorado State University, the University of Barcelona, and the Geisinger Obesity Institute, as indicated in the Results. Preparation of mouse liver homogenates (Holmstrom et al 2012), permeabilized cardiac and soleus muscle fibers (Li Puma et al 2020), and isolated mitochondria (Heim et al 2017; Li Puma et al 2020) were prepared a previously described in our cited publications. The livers from the FVB mice were homogenized using the Shredder SG3 (Pressure Biosciences) in MiR05 supplemented with ~ 5 µg/mL of digitonin. All respirometry experiments were performed on Oroboros O2k oxygraphs (Oroboros Instruments, Innsbruck, Austria) in MiR05 buffer containing 110 mM sucrose, 20 mM HEPES, 10 mM KH_2PO_4, 20 mM taurine, 20 mM lactobionic acid, 3 mM $MgCl_2$ $6H_2O$, 0.6 mM EGTA, 1 mg/ml bovine serum albumin. Standardized instrumental and chemical calibrations were applied using Datlab software for accurate measurement of chamber O_2 content and flux according to the manufacturer instructions, which includes corrections for background diffusion of oxygen into the chamber, the oxygen solubility in MiR05 (0.92), and background consumption of oxygen

by the electrodes across a broad range (50–450 μM) of chamber O_2 concentrations. Sample mitochondrial J_{O_2} was monitored in real-time by resolving changes in the negative time derivative of the chamber oxygen concentration, normalized to the protein content (mitochondria) or tissue mass (fibers and homogenates) added to the chamber.

3. Results and Discussion

3.1. "Rotenone Paradox" reveals complex interaction of CI and CII during multi-substrate respirometry protocols

One of the most important innovations afforded by HRR is the design and interpretation of multi-substrate titration protocols, which enable users to investigate the contributions of individual substrate oxidation pathways and electron transferring complexes to the observed J_{O_2} in a single sample experiment. Oxidation of malate, glutamate, and pyruvate directly produce NADH, so they are routinely considered to be "CI-linked" or N-pathway substrates representing the oxidation of carbohydrates (PM; pyruvate + malate), glutamate directly (via glutamate dehydrogenase), malate-aspartate shuttle flux (GM; glutamate + malate), or a combination of all three (PGM) (Gnaiger 2020). The contribution of CII is typically thought to be minimal during these N-pathway states due to the interaction of exogenous substrate concentrations with endogenous TCA cycle enzymes and intermediates, particularly in the presence of malate (Figure 2) (Gnaiger 2020). Malate supports NADH production by malate dehydrogenase while also generating oxaloacetate (OAA) needed for the production of citrate and 2-oxoglutarate to support PM and GM flux, respectively (Figure 2). However, OAA is also a potent inhibitor of CII (Fink et al 2018). OAA may accumulate if its production from malate exceeds its removal by downstream enzymes (citrate synthase, aspartate amino-transferase, and perhaps others). Malate can also feedback inhibit fumarase to favor cataplerosis of succinate, as well as 2-oxoglutarate and citrate through inner membrane antiporter when administered at millimolar concentrations, further limiting TCA cycle flux through CII (Dolce et al 2014). Consequently, N-pathway flux supported by PM, GM, and PGM is routinely interpreted as a specific measure of CI-supported J_{O_2} (Gnaiger 2020).

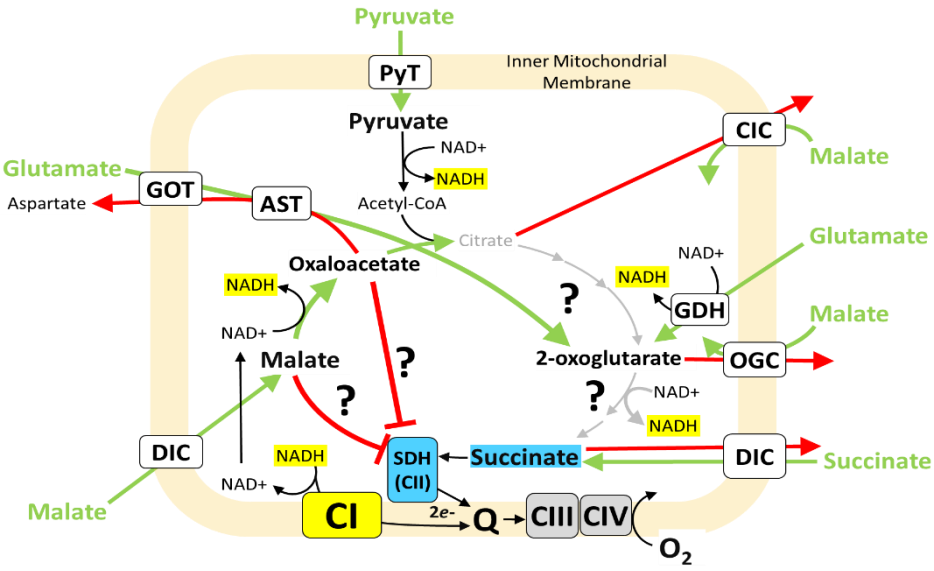

Figure 2. Potential impact of anaplerotic and cataplerotic pathways on CAC flux in the NS-pathway. During multi-substrate titration protocols, the addition of exogenous substrates at millimolar concentrations results in a complex interaction of anaplerotic, cataplerotic, and feedback/allosteric inhibition reactions that complicate interpretation of N and S pathway flux. AST, aspartate aminotransferase; CIC, mitochondrial citrate:malate exchanger; DIC, dicarboxylate transporter; GDH, glutamate dehydrogenase; GOT, glutamate:aspartate antiporter; OGC, oxoglutarate:malate antiporter; PyT, pyruvate transporter; SDH, succinate dehydrogenase; Q, ubiquinone; "?", unclear/variable contributions.

Titrating high millimolar concentrations of succinate to mitochondria oxidizing N-pathway substrates can overcome these limitations on CII-supported J_{O_2}, thus enabling the maximal NS-pathway J_{O_2} supported by reconstitution of forward TCA cycle flux and convergent electron flow to the ETS through CI and CII (Gnaiger 2020). Under these conditions, it is common to add the specific CI inhibitor rotenone to investigate the contribution of CI to the collective NS-pathway flux. Using simple math, the contributions of N and S pathways can be e by a variety of flux control factors (Pesta, Gnaiger 2012), essentially modeled on the assumption that rotenone decreases J_{O_2} by the proportion of NS-pathway flux contributed by CI (N), such that (N+S) – N = S; and therefore, (N+S)-S = N. Substrate control factors can also be calculated during the sequential titration of N and S substrates in the absence of inhibitors, which are generally assumed to provide the same information. However, those familiar with such protocols have likely noticed that the calculated contributions of N and S to the collective NS flux can differ depending on which approach is used, suggesting a more complex interaction of N and S substrate oxidation than simply the convergent flow of electrons from CI and CII to Q in the ETS.

Perhaps the most dramatic example of this is the "rotenone paradox", first presented (to our knowledge) by Dr. Brian Irving at a Mitochondrial Physiology conference in 2013, which demonstrated an increase in NS-pathway-supported J_{O_2} in mouse liver homogenates following the addition of rotenone. The phenomenon was reproduced by at least two independent laboratories in samples from FVB and C57Bl/6J mice, and found to be specific to liver mitochondria oxidizing GM as the N-pathway substrates (Figure 3A). However, in both cardiac (Figure 3B) and skeletal muscle (Figure 3C) permeabilized

fibers, the calculated contribution of the N-pathway (GM) to the collective NS flux following the addition of rotenone (Figure 3, N%$_2$) was still less than the recorded N-pathway flux before the addition of succinate (Figure 3, N%$_1$).

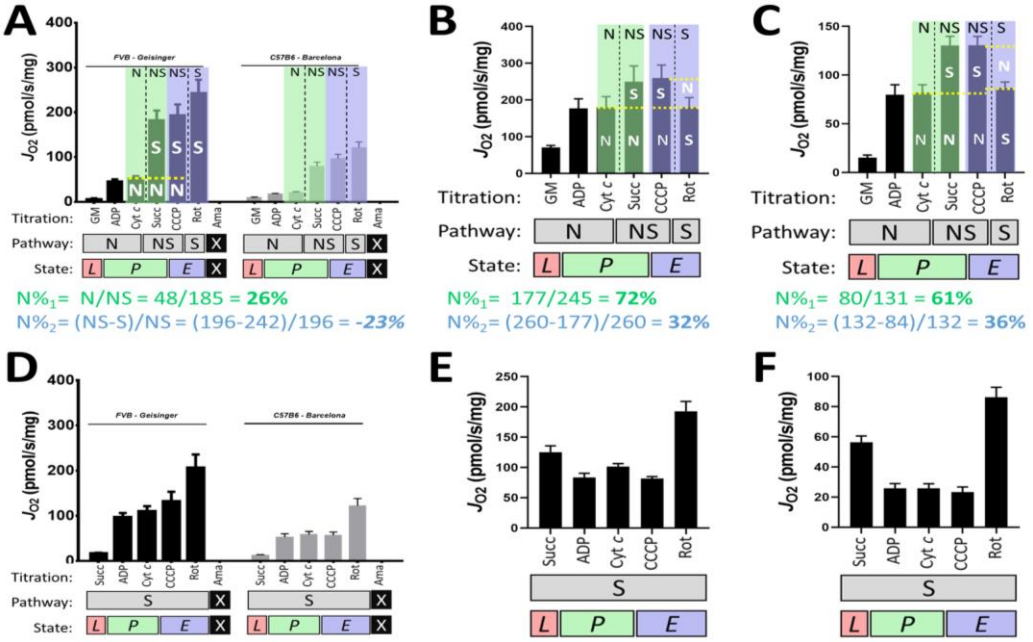

Figure 3. The "rotenone paradox". A) Oxygen consumption rates (J_{O_2}) of liver homogenates (0.8-2 mg) from FVB mice housed at Geisinger and C57Bl/6 mice in Barcelona demonstrating a paradoxical increase in GMS-supported NS-pathway flux following the addition of the CI-inhibitor rotenone (0.5 µM). In permeabilized cardiac muscle fibers (B) and soleus muscle fibers (C) from C57Bl/6 mice in Colorado, rotenone inhibited GMS-supported J_{O_2}, but the contribution of N-pathway flux predicted by this inhibition (N%$_2$) was ~40–50 % less than by titration of N-pathway substrates prior to succinate (N%$_1$). When succinate is used as the sole substrate (S-pathway flux), rotenone markedly increases in J_{O_2} in liver homogenates (D), cardiac (E) and soleus fibers (F). Notably, experiments in D-F also demonstrate a decrease in S-pathway flux following the addition of ADP in muscle and heart (the "succinate paradox" (Komlodi et al 2017; Doerrier et al 2015)), but not liver mitochondria. Data are means ± SD; *N*=3–4/group. CCCP, 1–3 µM carbonyl cyanide m-chlorophenyl hydrazine (protonophore uncoupler). *E*, non-coupled maximal J_{O_2}; *P*, OXPHOS-linked J_{O_2} in the presence of 2.5–5.0 mM ADP; PGM, 5 mM pyruvate, 10 mM glutamate, 1–2 mM malate; cyt c, 10–20 µM cytochrome *c*; N, NADH-linked J_{O_2} state; S, succinate-linked J_{O_2} state; *L*, proton leak-associated J_{O_2}; X, 2.5–7.5 µM antimycin.

As reported previously by the Garcia-Roves group (Holmstrom et al 2012), when pyruvate was added in conjunction with glutamate (PGM) before the addition of succinate, rotenone led to an expected decrease in all three tissues, but the calculated N%$_2$ was still only ~50 % of N%$_1$ calculated by substrate titration (Supplemental Figure 1). Similar results were obtained when PMS were used as substrates before the addition of rotenone in liver homogenates and mitochondria isolated from heart and skeletal muscle (data not shown). Taken together, these results demonstrate that CI activity in some way limits the contribution of succinate oxidation to NS-pathway flux in a substrate- and tissue-specific manner, such that rotenone reveals a greater S-pathway flux than is

predicted by subtracting the initial N from the subsequent NS-supported J_{O_2}. In addition, these results could indicate that endogenous succinate oxidation contributes to J_{O_2} supported by N-pathway substrates, such that the addition of rotenone reveals the authentic contribution of N-pathway flux to NS-supported J_{O_2} (N%2).

Inhibition of CI is well-known to be required for obtaining stable J_{O_2} from mitochondrial preparations oxidizing succinate in the absence of pyruvate or glutamate to prevent inhibitory accumulation of malate and OAA (Chance, Hagihara 1962; Fink et al 2018; Fink et al 2019; Harris, Manger 1968). This is because malate dehydrogenate requires NADH oxidation (regeneration of NAD^+ by CI) to catalyze its conversion to OAA. This phenomenon is demonstrated by an increase in J_{O_2} following the addition of rotenone to liver, cardiac and muscle mitochondria oxidizing succinate alone (Figure 3D-F). We hypothesize that the "rotenone paradox" reflects a similar limitation of succinate-supported oxidation by malate and/or OAA accumulation in the presence of NS-pathway substrates, which is subsequently revealed by inhibition of CI-linked malate oxidation (Figure 4). Notably, the magnitude of this effect varies across tissues, consistent with earlier evidence for variations in the relative activities of TCA cycle enzymes and anaplerotic/cataplerotic flux that contribute to NS pathway flux (Harris, Manger 1968). Consequently, we predicted that such processes might also impact J_{O_2} supported by N-pathway substrates alone in a tissue- and substrate-specific manner, which was investigated by the following experiments.

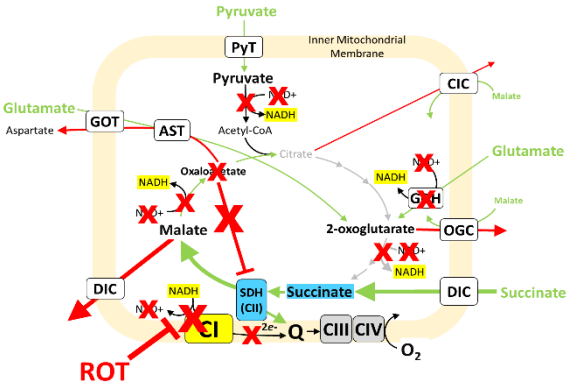

Figure 4. Hypothetical explanation for the "rotenone paradox". Inhibition of complex I with rotenone prevent oxidation of NADH, thus inhibiting activity of enzymes that require oxidized NAD+ for catalytic activity (red "X"s).

3.2. Tissue-specific influence of malate concentration on N-pathway supported J_{O_2} in isolated mitochondria.

The interactions proposed to explain the rotenone paradox above are likely to be sensitive to the malate concentrations titrated and are perhaps tissue-specific, as discussed elsewhere (Fink et al 2018; Fink et al 2019; Harris, Manger 1968). Therefore, we predicted that malate concentration might also impact the contribution of CII to J_{O_2} supported by conventional N-pathway substrates in the absence of succinate in a substrate- and tissue-specific manner. To test this, we first determined the effect of increasing malate concentrations on OXPHOS-linked J_{O_2} (in the presence of 2.5 mM ADP) supported by pyruvate (5 mM) and/or glutamate (5 mM) in C57Bl/6 mouse liver, muscle and cardiac mitochondria in the absence of succinate. As predicted and previously suggested by Gnaiger (Gnaiger 2020), malate concentrations above 0.5 mM inhibited N-pathway J_{O_2} supported by GM, PM, or PGM in a concentration- and tissue-dependent manner (Figure 5). In the GM-supported N-state (5 mM glutamate + 0.5 mM malate), a generally linear inhibition of mitochondrial J_{O_2} was seen in all three tissues above 1 mM, with approximately 50 % inhibition of flux at 5 mM (Figure 5A). Interestingly, 2.5 mM

titrations of succinate led to a potent linear recovery of J_{O_2} in liver and heart mitochondria, which exceeded initial N-pathway rates at 5 mM in liver, and 15 mM in heart. Conversely, no significant recovery was seen in skeletal muscle mitochondria even after the titration of 25 mM succinate.

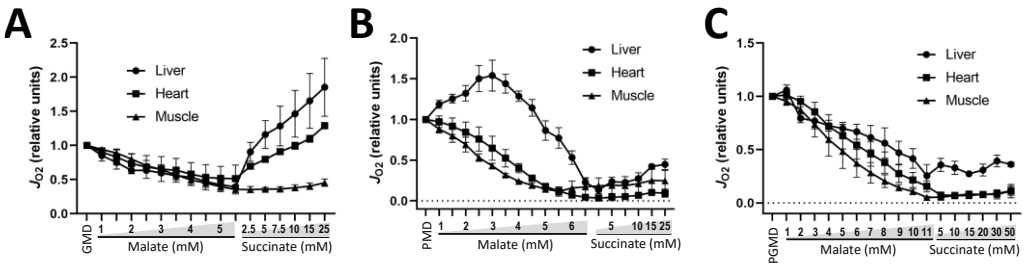

Figure 5. Tissue-specific inhibition of >1 mM malate concentration on N-State J_{O_2}. Relative changes in oxygen consumption rate (J_{O_2}) of mitochondria isolated from mouse liver (60 µg protein), heart and muscle (30 µg protein) in response to serial titration of malate beginning from a basal OXPHOS-linked respiration state (with 2.5 mM ADP) supported by 5 mM glutamate + 0.5 mM malate (A; GM), 5 mM pyruvate + 0.5 malate (B; PM) or 5 mM glutamate + 5 mM pyruvate + 0.5 mM malate (C; PMG), followed by titration of succinate. Data are means ± SD; N=3–4/group.

In the PM-supported N-state (5 mM pyruvate + 0.5 mM malate), a similar but more potent inhibition of J_{O_2} was observed with malate concentrations above 1 mM in cardiac and muscle mitochondria, with minimal recovery following succinate titrations up to 25 mM (Figure 5B). However, malate concentrations increased PM-linked flux in liver mitochondria up to 3 mM, above which flux declined steeply to near zero by 6.5 mM, with only partial recovery of flux with 25 mM succinate.

In the PGM-supported N-state (5 mM pyruvate + 5 mM glutamate + 0.5 mM malate), malate concentrations above 1 mM led to generally linear decreases in J_{O_2} that were most potent in muscle > heart > liver mitochondria (Figure 5C). Full inhibition of J_{O_2} was seen in muscle and heart mitochondrial above 11 mM malate, while liver mitochondria maintained ~25 % of basal flux at this concentration. In all three tissue mitochondria, titration of succinate up to 50 mM resulted in only a minimal recovery of flux in the presence of 11 mM malate.

Taken together, these studies demonstrate marked tissue-specific effects of malate concentration on N-pathway flux that vary depending on whether pyruvate or glutamate are used as substrates. Similar variations in the ability of succinate to overcome these concentrations suggest tissue-specific variations in OAA metabolism/accumulation or sensitivity of CII to OAA inhibition. There are several possible explanations and conclusions that could be drawn from these results, which are discussed below and open for comment, revision, and additions:

1) The inhibition of GM-supported flux by malate in all 3 tissues suggests that succinate oxidation contributes significantly to J_{O_2} in this "N-pathway" state when malate concentration is low. Despite being conventionally viewed at exclusively CI-linked, GM oxidation enables the flow of electrons from both CI and CII contributed by malate dehydrogenase (MDH), 2-oxoglutarate dehydrogenase (OGD), CII, and glutamate dehydrogenase (GDH), facilitating substrate flow from malate→OAA→2-oxoglutarate→succinate→malate.

2) The inhibition of PM-supported flux by malate in all 3 tissues suggests that succinate oxidation also contributes significantly to J_{O_2} in this N-pathway state when malate concentration is low. PM oxidation at the concentrations used herein results in at least partial forward flux of the TCA cycle through succinate dehydrogenase as depicted in Figure 1A. However, higher malate concentrations increasingly favors feedback inhibition of fumarase (and CII), and cataplerosis (antiport) of both citrate (Catalina-Rodriguez et al 2012) and 2-oxoglutarate (Palmieri et al 1993). The latter progressively decreases NADH production from isocitrate dehydrogenase (IDH) and ODH, further limiting succinate production oxidation by CII downstream and consequently reducing the observed J_{O_2}.

3) An increasing concentration of malate favors greater cataplerosis of 2-oxoglutarate, which increasingly limits its oxidation by OGD, thus decreasing NADH production and succinate oxidation downstream. Higher malate concentrations favor feedback inhibition of fumarase, and thus CII, further promoting cataplerosis of 2-oxoglutarate (Palmieri et al 1993) and succinate (Dolce et al 2014) and loss of electrons supplied by their oxidation. Higher malate concentrations might also favor the accumulation of OAA and inhibition of CII as discussed above, particularly as concentrations approach those of glutamate that is needed to convert OAA to 2-oxoglutarate. This may be particularly relevant in skeletal muscle, where 25 mM succinate was insufficient to overcome 6 mM malate, but less so in the heart and liver, where succinate titration fully recovers J_{O_2} at 5−15 mM.

4) The transient increase in PM-supported J_{O_2} with malate concentrations up to 3 mM in liver mitochondria reflects improved clearance of OAA compared to heart and skeletal muscle. The liver relies heavily on mitochondrial phosphoenolpyruvate carboxykinase (mPEPCK) for gluconeogenesis, which contributes significantly to OAA cataplerosis in hepatocytes (Stark et al 2014) as well as pancreatic islet cells (Stark et al 2009). In addition, mPEPCK regenerates guanosine diphosphate (GDP) utilized by succinyl-CoA ligase to produce succinate, thereby potentially regulating TCA cycle flux from OGD to succinate dehydrogenase (Stark et al 2014; Stark, Kibbey 2014; Stark et al 2009). Accordingly, a greater abundance of mPEPCK in liver compared to heart and muscle mitochondria may both attenuate OAA accumulation and facilitate succinate production in respirometry protocols using N-pathway substrates. However, the liver also expresses much greater levels of pyruvate carboxylase than heart and skeletal muscle (www.proteinatlas.org/ENSG00000173599-PC/tissue), which generates OAA from pyruvate, potentially explaining the more robust "rotenone paradox" in liver oxidizing GM compared to PM as N-pathway substrates. We hypothesize that the activity of these enzymes may accounts for some of the biological variation observed between tissues in multi-substrate respirometry protocols, ultimately by regulating the contribution of succinate oxidation to J_{O_2} supported by N-pathway substrates.

3.3. Malonate inhibits N-pathway flux in a tissue- and substrate-specific manner.

Based on the conclusions above, we next tested the hypothesis that CII contributes significantly to N-pathway flux supported by GM, PM, and PGM oxidation, utilizing 4 mM malonate as a specific inhibitor of succinate dehydrogenase following the addition of ADP in the same malate-titrations protocols used above. As predicted, malonate inhibited OXPHOS-linked J_{O_2} supported by GM, PM, and PMG in a tissue- and substrate-specific manner (Figure 6).

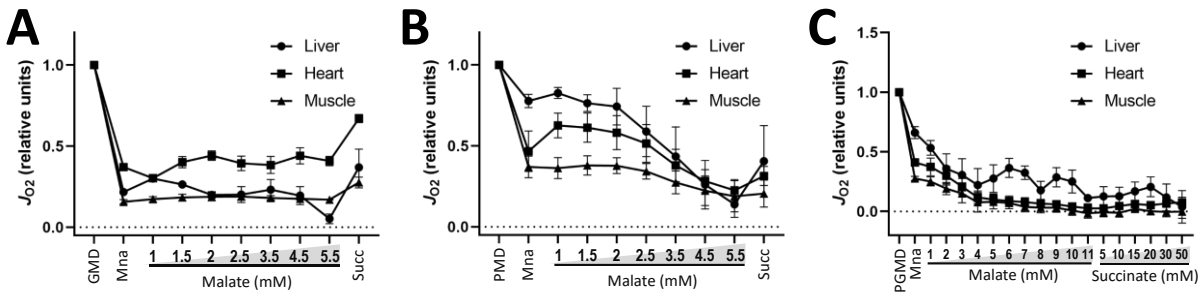

Figure 6. Malonate inhibits N-State J_{O_2} in a tissue- and substrate-specific manner. Relative changes in oxygen consumption rate (J_{O_2}) of mitochondria isolated from liver (60 µg protein), heart and muscle (30 µg protein) in response to inhibition of CII with malonate (4 mM), followed by serial titration of malate (1–11 mM), beginning from a basal OXPHOS-linked respiration state (with 2.5 mM ADP) supported by 5 mM glutamate + 0.5 mM malate (A; GM), 5 mM pyruvate + 0.5 malate (B; PM) or 5 mM glutamate + 5 mM pyruvate + 0.5 mM malate (C; PMG), followed by titration of succinate (5–50 mM). Data are means ± SD; N=3–4/group.

In the GM-supported N-state (5 mM glutamate + 0.5 mM malate), malonate inhibited J_{O_2} at least 50 % in mitochondria from all three tissues (Figure 6A), largely negating the inhibitory effects of the malate titration observed in Figure 5A. Interestingly, malate titration induced a partial recovery J_{O_2} in cardiac mitochondria, perhaps indicating a greater capacity for GM-supported malate-aspartate shuttle flux in the presence of CII-inhibition. Partial recovery of J_{O_2} was seen in all 3 mitochondria following the addition of 25 mM succinate, consistent with malonate being a competitive inhibitor of CII, which was reversed by titration of 5-15mM malonate (data not shown).

In the PM-supported N-state (5 mM pyruvate + 0.5 mM malate), a less robust inhibition of J_{O_2} was seen following the addition of malonate (Figure 6B), with the greatest effect seen in muscle > heart > liver, consistent with the effects of malate titration in Figure 5B. Interestingly, subsequent titration of > 2 mM malate resulted in additional inhibition of flux, perhaps reflecting reduced contributions of NADH from ICDH and ODH due to increasing cataplerosis of citrate and oxo-glutarate driven by malate antiport. Greater inhibition of CII flux seems less likely given the partial recovery of J_{O_2} following the addition of 25 mM succinate, though we cannot rule out contributions of reduced CII flux due to OAA accumulation during the preceding malate titration.

In the PGM-supported N-state (5 mM pyruvate + 5 mM glutamate + 0.5 mM malate), malonate inhibited J_{O_2} in muscle > heart > liver as seen in with PM and GM alone (Figure 6C), consistent with the trends observed following malate titration in Figure 5C. However, subsequent titration of 5 mM malate nearly completely inhibited J_{O_2} in muscle and heart mitochondria, while the liver was more resistant, with no recovery of flux after the addition of 50 mM succinate in mitochondria in all 3 tissues.

Taken together, the results of these experiments support the conclusions derived from the malate titration experiments above, most notably that there is a significant contribution of CII (succinate oxidation) to J_{O_2} supported by N-pathway substrates in liver, heart, and muscle mitochondria. The extent of this contribution observed in multi-substrate respirometry protocols likely depends on the malate concentration used, which potently limits oxidation of both succinate and TCA cycle intermediates through the

mechanisms discussed above and illustrated in Figure 2. Consequently, variations in the relative protein expression and K_{eq} of cataplerotic and dehydrogenase enzymes across tissues and conditions may account for important differences in mitochondrial J_{O_2} supported by N and NS-pathway substrates. Further exploration of how modulators of OAA cataplerosis (e.g., mitochondrial PEPCK and aspartate aminotransferase), oxo-glutarate metabolism, and succinyl-CoA ligase activity influence J_{O_2} during multi-substrate respirometry protocols may provide further insights and opportunities for using high-resolution respirometry to elucidate changes in diverse metabolic processes upstream of the ETS. We welcome the comments, perspectives and experimentation of others along these lines, particularly within the contexts of relevant biological stressors and/or disease processes that may impact these pathways.

Abbreviations

AST	Asapartate amniotrasferase	N-pathway	NADH-producing pathway
CI/II	Complex I/II	OAA	oxaloacetate
DIC	Dicarboxylate transporter	S-pathway	Succinate oxidation
J_{O_2}	Oxygen consumption rate	TCA	Tricarboxylic acid

Acknowledgements

The authors acknowledge the insights and discussions of Dr. Erich Gnaiger and the MitoEAGLE working group members for providing the intellectual foundation for these studies and what we hope will be an ongoing effort to elucidate the biochemical bases for variations in multi-substrate respirometry protocols. We also thank Dr. George Argyropoulos and Steve Roesch for providing the FVB livers.

References

Catalina-Rodriguez O, Kolukula VK, Tomita Y, Preet A, Palmieri F, Wellstein A, Byers S, Giaccia AJ, Glasgow E, Albanese C, Avantaggiati ML (2012) The mitochondrial citrate transporter, CIC, is essential for mitochondrial homeostasis. Oncotarget 1220-35. https://doi.org/10.18632/oncotarget.714

Chance B, Hagihara B (1962) Activation and inhibition of succinate oxidation following adenosine diphosphate supplements to pigeon heart mitochondria. J Biol Chem 3540-5.

Doerrier C, Plangger I, Sumbalova Z, Fasching M, Tretter L & Gnaiger E (2015) "Succinate paradox" study by high resolution respirometry combined with fluorometry and spectrofluorometry: NextGen-O2k. MiPschool Greenville 2015.

Dolce V, Cappello AR, Capobianco L (2014) Mitochondrial tricarboxylate and dicarboxylate-tricarboxylate carriers: from animals to plants. IUBMB Life 462-71. https://doi.org/10.1002/iub.1290

Fink BD, Bai F, Yu L, Sheldon RD, Sharma A, Taylor EB, Sivitz WI (2018) Oxaloacetic acid mediates ADP-dependent inhibition of mitochondrial complex II-driven respiration. J Biol Chem 19932-19941. https://doi.org/10.1074/jbc.RA118.005144

Fink BD, Yu L, Sivitz WI (2019) Modulation of complex II-energized respiration in muscle, heart, and brown adipose mitochondria by oxaloacetate and complex I electron flow. FASEB J. 11696-11705. https://doi.org/10.1096/fj.201900690R

Gnaiger E (2020) Mitochondrial pathways and respiratory control. An introduction to OXPHOS analysis. 5th ed. Bioenerg Commun 2020.2. https://doi.org/10.26124/bec:2020-0002

Harris EJ, Manger JR (1968) Intramitochondrial substrate concentration as a factor controlling metabolism. The role of interanion competition. Biochem J 239-46. https://doi.org/10.1042/bj1090239

Heim AB, Chung D, Florant GL, Chicco AJ (2017) Tissue-specific seasonal changes in mitochondrial function of a mammalian hibernator. Am J Physiol Regul Integr Comp Physiol R180-R190. https://doi.org/10.1152/ajpregu.00427.2016

Holmstrom MH, Iglesias-Gutierrez E, Zierath JR, Garcia-Roves PM (2012) Tissue-specific control of mitochondrial respiration in obesity-related insulin resistance and diabetes. Am J Physiol Endocrinol Metab E731-9. https://doi.org/10.1152/ajpendo.00159.2011

Komlodi T, Horvath G, Svab G, Doerrier C, Sumbalova Z, Tretter L, Gnaiger E (2017) Succinate dehydrogenase regulation via oxaloacetate in brain mitochondria. MitoEAGLE Barcelona 2017.

Li Puma LC, Hedges M, Heckman JM, Mathias AB, Engstrom MR, Brown AB, Chicco AJ (2020) Experimental oxygen concentration influences rates of mitochondrial hydrogen peroxide release from cardiac and skeletal muscle preparations. Am J Physiol Regul Integr Comp Physiol R972-R980. https://doi.org/10.1152/ajpregu.00227.2019

Palmieri F, Bisaccia F, Capobianco L, Dolce V, Fiermonte G, Iacobazzi V, Zara V (1993) Transmembrane topology, genes, and biogenesis of the mitochondrial phosphate and oxoglutarate carriers. J Bioenerg Biomembr 493-501. https://doi.org/10.1007/BF01108406

Pesta D, Gnaiger E (2012) High-resolution respirometry: OXPHOS protocols for human cells and permeabilized fibers from small biopsies of human muscle. Methods Mol Biol 25-58. https://doi.org/10.1007/978-1-61779-382-0_3

Stark R, Guebre-Egziabher F, Zhao X, Feriod C, Dong J, Alves TC, Ioja S, Pongratz RL, Bhanot S, Roden M, Cline GW, Shulman GI, Kibbey RG (2014) A role for mitochondrial phosphoenolpyruvate carboxykinase (PEPCK-M) in the regulation of hepatic gluconeogenesis. J Biol Chem 7257-63. https://doi.org/10.1074/jbc.C113.544759

Stark R, Kibbey RG (2014) The mitochondrial isoform of phosphoenolpyruvate carboxykinase (PEPCK-M) and glucose homeostasis: has it been overlooked? Biochim Biophys Acta 1313-30. https://doi.org/10.1016/j.bbagen.2013.10.033

Stark R, Pasquel F, Turcu A, Pongratz RL, Roden M, Cline GW, Shulman GI, Kibbey RG (2009) Phosphoenolpyruvate cycling via mitochondrial phosphoenolpyruvate carboxykinase links anaplerosis and mitochondrial GTP with insulin secretion. J Biol Chem 26578-90. https://doi.org/10.1074/jbc.M109.011775

Supplemental Figures

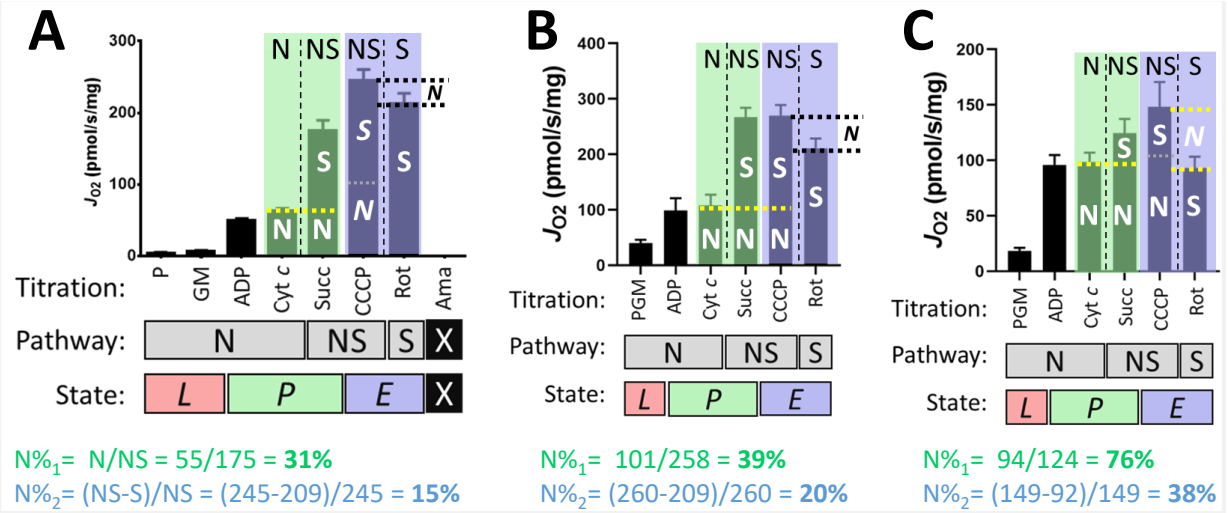

$N\%_1$= N/NS = 55/175 = **31%**
$N\%_2$= (NS-S)/NS = (245-209)/245 = **15%**

$N\%_1$= 101/258 = **39%**
$N\%_2$= (260-209)/260 = **20%**

$N\%_1$= 94/124 = **76%**
$N\%_2$= (149-92)/149 = **38%**

Supplemental Figure S1. Less than expected decrease in J_{O_2} following rotenone titration in the PGMS-supported NS-state. Oxygen consumption rate (J_{O_2}) of liver homogenates (0.8–2 mg) from FVB mice (A), and permeabilized cardiac muscle fibers (B) and soleus muscle fibers (C) from C57Bl/6 mice demonstrating a lower contribution of N-pathway flux to NS-supported J_{O_2} predicted by 0.5 µM rotenone inhibition ($N\%_2$) than the J_{O_2} supported by N-pathway substrates prior to the addition of succinate ($N\%_1$). Data are means ± SD; *N*=3–4/group. CCCP, 1–3 µM carbonyl cyanide m-chlorophenyl hydrazine (protophore uncoupler). *E*, non-coupled maximal J_{O_2}; *P*, OXPHOS-linked J_{O_2} in the presence of 2.5–5 mM ADP; PGM, 5 mM pyruvate, 10 mM glutamate, 1–2 mM malate; cyt c, 10–20 µM cytochrome *c*; N, NADH-linked J_{O_2} state; S, succinate-linked J_{O_2} state; *L*, proton leak-associated J_{O_2}; X, 2.5–7.5 µM antimycin.